

EFFECTS OF TIME AND TEMPERATURE ON THE FORMATION
OF CORDIERITE FROM VARIOUS RAW MATERIALS

A THESIS

Presented to

The Faculty of the Division of Graduate Studies

By

James R. Storey

In Partial Fulfillment
of the Requirements for the Degree
Master of Science in Ceramic Engineering

Georgia Institute of Technology

December, 1975

EFFECTS OF TIME AND TEMPERATURE ON THE FORMATION
OF CORDIERITE FROM VARIOUS RAW MATERIALS

Approved:

[Signature]

Joe K. Cochran, Jr. Chairman

[Signature]

W. I. Pentecost

[Signature]

James F. Benzel

Date approved by Chairman: 12/4/75

ACKNOWLEDGMENTS

I am deeply indebted to Dr. Joe K. Cochran, Jr. for his guidance and assistance in this work. My appreciation is expressed to Dr. J. S. Pentecost for his interest and for serving on my reading committee. My appreciation is also expressed to Dr. James F. Benzel for serving on my reading committee.

I wish to thank Mr. Thomas Mackrovitch for his cheerful help in the preparation of the raw materials and the blending of the bodies.

TABLE OF CONTENTS

	Page
ACKNOWLEDGMENTS.	ii
LIST OF TABLES	v
LIST OF ILLUSTRATIONS.	vi
SUMMARY.	viii
Chapter	
I. INTRODUCTION.	1
II. SURVEY OF LITERATURE.	3
Cordierite Crystal Structure.	3
Silica-Alumina-Magnesia Ternary System.	4
Physical Properties	6
Solid State Reaction Kinetics	6
III. PROCEDURE	12
Body Preparation and Firing	12
Quantitative Phase Analysis	13
Internal Standard Theory	
Preparation of Standard Curves	
Quantitative Phase Analysis of Unknowns	
IV. RESULTS AND DISCUSSION.	22
Reaction of Kaolin and Talc	22
Effects of Spinel Additions	
Reaction of Spinel-Silica	27
Comparison with Kaolin-Talc and Kaolin-	
Talc-Spinel	
Effects of Spinel Addition	
Comparison with Spinel-Silica	
Reaction Kinetics	41
V. CONCLUSIONS AND RECOMMENDATIONS	44
Conclusions	44
Recommendations	

TABLE OF CONTENTS (Concluded)

Appendices	Page
A. RAW MATERIALS	47
B. EXPERIMENTAL X-RAY DIFFRACTION SETTINGS	50
BIBLIOGRAPHY	51

LIST OF TABLES

Table		Page
1.	Composition of Cordierite Bodies.	10
2.	Raw Material Average Particle Size.	10
3.	Cordierite Body Raw Materials Compositions.	12
4.	Standard Body Compositions.	16
5.	X-Ray Peak Locations.	16
6.	Cordierite Weight Percent in Kaolin-Talc Body	23
7.	Mullite Weight Percent in Kaolin-Talc Body.	26
8.	Cordierite Weight Percent in Kaolin-Talc-Spinel Body.	27
9.	Cordierite Weight Percent in Spinel-Silica Body	30
10.	Cordierite Weight Percent in Spinel-Silica- Excess Spinel	37
11.	Cordierite Weight Percent in Alumina-Silica- Magnesia.	39
12.	Jander Activation Energy.	43
13.	Raw Materials Source.	47
14.	Raw Material Particle Size.	48
15.	Chemical Analysis of Edgar Plastic Kaolin	49
16.	Experimental X-Ray Diffraction Settings	50

LIST OF ILLUSTRATIONS

Figure	Page
1. Alumina-Magnesia-Silica Ternary System.	5
2. Model for the Reaction of a Sphere of Component A with Component B.	8
3. Cordierite Calibration Curve (29.5° Peak)	18
4. Mullite Calibration Curve	19
5. Corrected Alumina Calibration Curve	20
6. Effect of Time and Temperature on Cordierite Content of Kaolin-Talc Body (Composition 1)	24
7. Effect of Time on Cordierite Content of Kaolin-Talc Body (Composition 1) at 1350°C and 1400°C and Kaolin-Talc-Spinel Body (Composition 4) at 1400°C	28
8. Effect of Time and Temperature on Cordierite Con- tent of Kaolin-Talc-Spinel Body (Composition 4)	29
9. Effect of Time and Temperature on Cordierite Content of Spinel-Silica Body (Composition 2)	31
10. Effect of Time on Cordierite Formation from Various Initial Raw Material Compositions at 1250°C	32
11. Effects of Time on Cordierite Formation from Various Initial Raw Materials at 1300°C	34
12. Effects of Time on Cordierite Formation from Various Initial Raw Materials Compositions at 1350°C.	35
13. Effects of Time on Cordierite Formation from Various Initial Raw Material Compositions at 1400°C	36
14. Effect of Time and Temperature on Cordierite Con- tent of Spinel-Silica-Excess Spinel Body (Com- position 5)	38
15. Effect of Time and Temperature on Cordierite Con- tent of Alumina-Magnesia-Silica Body (Composition 3).	40

LIST OF ILLUSTRATIONS (Concluded)

Figure	Page
16. $\log K_J$ versus $1/T^\circ K$ for Bodies 2, 3, and 5.	42

SUMMARY

Ceramic bodies which contain a high percentage of cordierite are coming more into use because of the low thermal expansion and high thermal shock resistance given to the body by the cordierite.

It was the purpose of this thesis to investigate the rate of formation of cordierite in five bodies, whose overall oxide composition was stoichiometric or near stoichiometric cordierite.

The five bodies were fired at temperatures of 1250, 1300, 1350, and 1400°C for times of 1, 5, 10, 15, and 20 hours. The cordierite and mullite contents of these bodies were then determined by quantitative x-ray analysis using rutile as an internal standard.

Cordierite was found to form more rapidly in clay-talc bodies than in spinel-silica and alumina-magnesia-silica bodies at lower temperatures. At higher temperatures the reverse was true. It appears the formation of cordierite in kaolin-talc bodies involves the presence of a liquid phase produced by localized melting which is detrimental to cordierite formation by solid state reaction, particularly at higher temperatures. The spinel-silica bodies and the alumina-magnesia-silica bodies were found to form cordierite at essentially the same rate at all temperatures.

CHAPTER I

INTRODUCTION

The market for ceramic bodies having high thermal shock resistance creates continual interest in low expansion bodies. One group of bodies receiving increased interest is those of or near the theoretical composition of cordierite, an incongruently melting compound in the Silica-Alumina-Magnesia phase diagram which forms at temperatures between 1100 and 1400°C. The quantity of crystalline cordierite is important to the thermal expansion coefficient, and therefore the thermal shock resistance of the bodies. However it is difficult to control the formation of cordierite in these bodies due to the narrow firing range in which cordierite forms rapidly. Underfiring the body fails to develop sufficient cordierite for low thermal expansion and high thermal shock resistance; whereas, overfiring causes deterioration of the cordierite content and an increase in the mullite and glassy phase content as well as increasing thermal expansion and lowering thermal shock resistance.

Two major factors affecting the commercial production of bodies containing crystalline cordierite are the cost of the raw materials and the availability of these materials. Two of the most commonly used raw materials are talc and clay, either calcined or uncalcined. In addition such materials as alumina, zircon, and magnesium carbonate are added to extend the firing range and improve the control over cordierite formation. Singer and Cohn (1) as early as 1929 reported on stoneware bodies having

unusually low thermal expansion. These were cordierite bodies made from clay, talc, and alumina. The recent demand for improved low expansion bodies has encouraged the use of more expensive, man made materials in the manufacture of cordierite. These materials do not contain the impurities found in natural raw materials. These impurities aggravate the problem of glass formation and often reduce both crystalline cordierite content and refractoriness of cordierite compositions.

It was the purpose of this work to investigate quantitatively the formation of cordierite in bodies of various initial composition over the temperature range of 1250 to 1400°C. The effect of oxide additions to certain bodies was also investigated. The Jander equation for solid state reactions was applied to the results and the activation energy calculated.

CHAPTER II

SURVEY OF LITERATURE

Cordierite Crystal Structure

The first study of the crystal structure of cordierite was carried out by Gossner and Mussgnug (2), who concluded that cordierite was orthorhombic and homotypic with beryl, having the structural formula $(\text{Mg}_2\text{Al})^{\text{IV}}\text{Al}_2^{\text{VI}}(\text{AlSi}_5)^{\text{IV}}\text{O}_{18}$. Bragg (3) later rewrote this formula as $\text{Al}_3\text{Mg}_2(\text{Si}_5\text{Al})\text{O}_{18}$ after consideration of the ionic radii.

Byström (4) in 1941 carried out a qualitative cordierite analysis confirming the homotypic relationship with beryl. He assigned a random distribution of one Al and five Si atoms to six member rings which he stressed in his drawing of the crystal structure viewed along the z axis. Byström's (4) arrangement was confirmed by a study conducted by G. V. Gibbs (5) which produced a more precise set of atomic parameters, indicating an ordered Al and Si arrangement.

Karkhanavala and Hummel (6) during a study of the cordierite-spodumene join proposed the existence of two stable (α and β) and one metastable (μ) modifications of cordierite. The α or high cordierite according to Schreyer and Schairer (7) is the first structure state to form at any temperature, but that after heating at appropriate temperatures the α form will go through a gradual transition to the β or low form. They indexed the x-ray pattern for α cordierite as that of a hexagonal unit cell having dimensions $a = 9.7698 \text{ \AA}$ and $c = 9.3517 \text{ \AA}$,

giving a theoretical density of 2.513. The β form they indexed as orthorhombic with dimensions of $a = 17.0621 \text{ \AA}$, $b = 9.7208 \text{ \AA}$, and $c = 9.3389 \text{ \AA}$ and a theoretical density of 2.507. According to Karkhanavala and Hummel (6) the β modification can be formed from α cordierite, metastable (μ) cordierite, and cordierite glass under hydrothermal conditions below 830°C . The metastable (μ) form appears if the glass is devitrified between 850 and 950°C , at ordinary pressure. Both β and μ forms will invert to the α form if heated to between 830 and 1050°C .

Miyashiro (8) proposed an alternative to this in which cordierite possesses a time dependent structural series between the hexagonal form and the orthorhombic form. He believed that the distortion in cordierite was a function of the structural state and the chemical composition.

Silica-Alumina-Magnesia Ternary System

Cordierite is a ternary compound in the $\text{SiO}_2\text{-Al}_2\text{O}_3\text{-MgO}$ ternary system. This ternary system is one of the more important industrial systems. In this system (Figure 1) appear the magnesite refractories, forsterite ceramics, steatites and low loss steatites, and cordierite ceramics. It contains two incongruently melting ternary compounds, cordierite and sapphirine, and four binary compounds. The lowest liquidus temperature is the eutectic temperature for the tridymite-protoenstatite-cordierite eutectic (1355°C) with the cordierite protoenstatite-forsterite eutectic temperature (1365°C) next. The point which corresponds to the theoretical composition of cordierite lies within the mullite primary phase region. This means that bodies near the theoretical composition for cordierite can be expected to have mullite present as a second phase,

Eutectic Temperature (°C)

A	1440
B	1460
C	1482
D	1578
E	1453
F	1370
G	1365
H	1355

No. Crystalline Phase

1	Cordierite
2	Mullite
3	Corundum
4	Spinel
5	Peridase
6	Forsterite
7	Protoenstatite
8	Silica (Tridymite and Cristobalite)
9	Two Liquids
10	Sapphirine

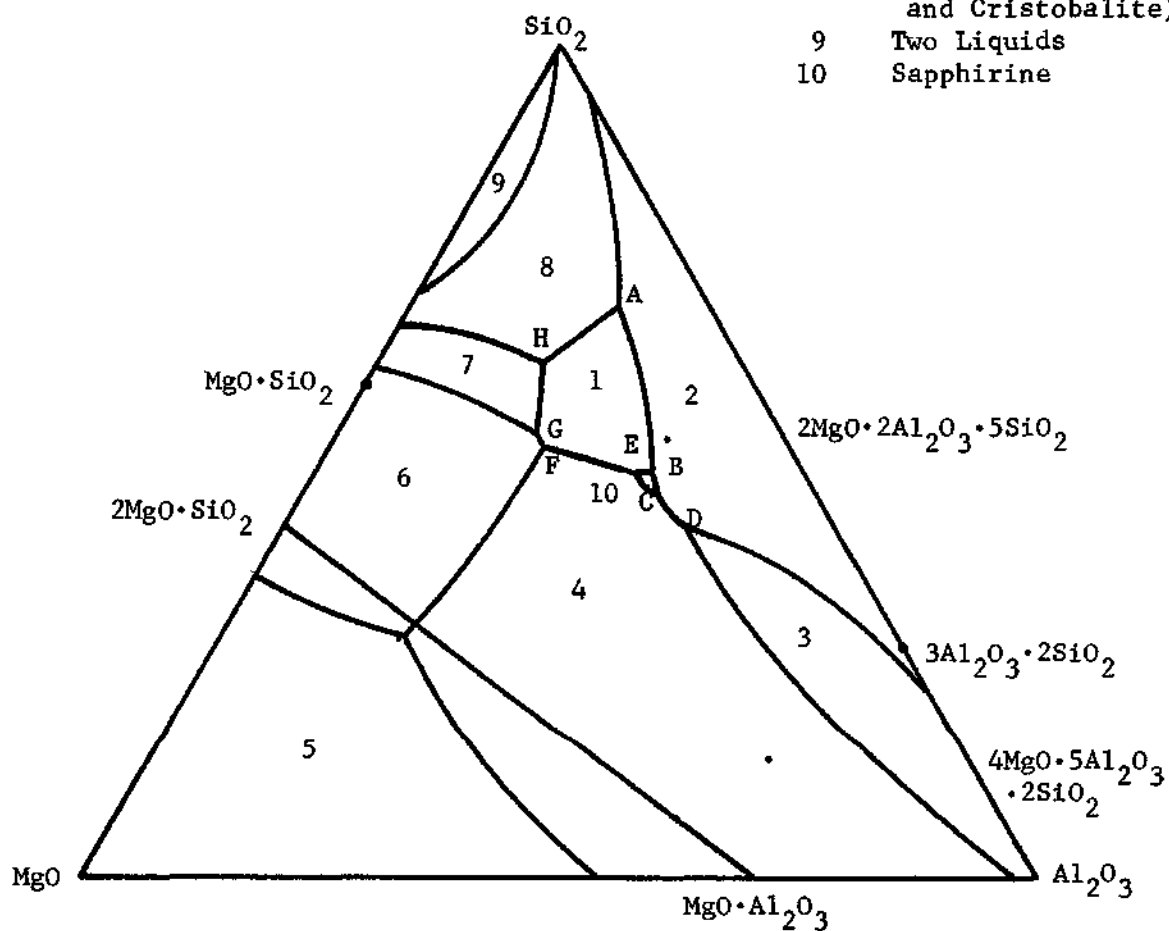


Figure 1. Alumina-Magnesia-Silica Ternary System

if the firing temperature and impurities are sufficient for liquid formation. The cordierite primary phase region itself is bounded by six invariant points which can be seen in Figure 1.

Physical Properties

One of the important properties of cordierite is its resistance to thermal shock, a partial result of its low thermal expansion. Karkhanavala and Hummel (6) reported a linear coefficient of thermal expansion of 47.2×10^{-7} °C over the range of 25 to 850°C for μ cordierite and a thermal expansion coefficient of 24.7×10^{-7} °C over the range of 25 to 1000°C for α cordierite. Beals and Cook (9) reported a coefficient of 12.5×10^{-7} over the range 20 to 300°C for a body containing 80 percent cordierite as determined by x-ray analysis and 10.2×10^{-7} over the same range for a body containing 97 percent crystalline cordierite.

A serious disadvantage to the use of cordierite is the narrow firing range it possesses. Underfiring fails to develop sufficient crystalline cordierite for low thermal expansion and high thermal shock resistance. Overfiring results in deterioration of crystalline cordierite into mullite and/or a glassy phase resulting in increased thermal expansion and lowered thermal shock resistance. The presence of these and other impurities in the cordierite body has a marked effect on thermal expansion. Lamar and Warner (10) have stated that mullite contents of less than five percent can increase the observed thermal expansion of cordierite by 100 percent in the low temperature region.

Solid State Reaction Kinetics

The formation of cordierite by current industrial techniques has

been assumed to be a solid state process. A number of models have been proposed to describe such solid state reactions. One of the models proposed by W. Jander (11) considered a sphere of material, A, having a radius, r . The sphere of A (Figure 2) was surrounded by a material, B, and the entire surface of A was considered to be reacting with B, giving a reaction product of thickness, y . Jander (11) assumed the rate of increase of y to be inversely proportional to y .

$$dy/dt = k/y \quad (1)$$

or

$$y^2 = 2kt \quad (2)$$

and the unreacted volume to be

$$V = (4/3)\pi(r-y)^3 \quad (3)$$

or

$$V = (4/3)\pi(r^3)(1-x) \quad (4)$$

where x is the fraction of the original sphere which has reacted. By equating the right hand side of both equations (3) and (4), Jander (11) arrived at an equation expressing y in terms of y and r .

$$y = r[1 - (1-x)]^{1/3} \quad (5)$$

By substituting equation (5) into equation (2) Jander (11) arrived at his solid state reaction equation:

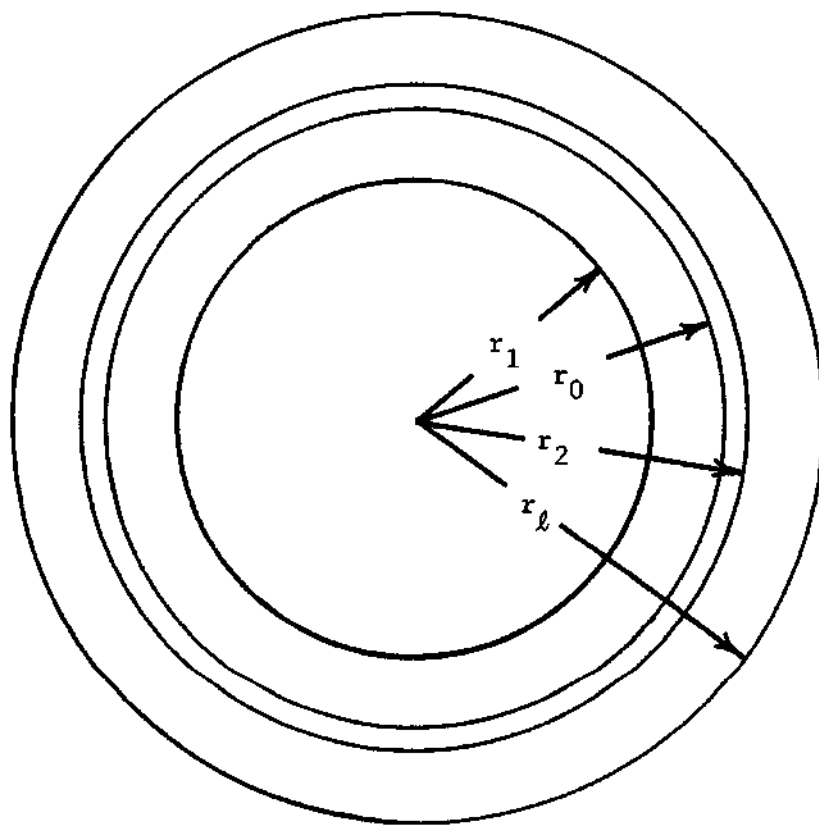


Figure 2. Model for the Reaction of a Sphere of Component A with Component B
(r_0 = initial radius of A; r_1 = instantaneous radius of A; r_ℓ = radius of product at $x = 1.0$; r_2 = instantaneous radius of unreacted A plus product)

$$[1 - (1-x)^{1/3}]^2 = \frac{2kt}{r^2} = Kt \quad (6)$$

Carter (12) in a critical analysis of the Jander (11) equation pointed out certain weaknesses in its development. The initial equation, equation (1), is for reaction of plane surfaces and would be valid only for values of x where the ratio of the inner and outer reaction surface areas is near unity. Equations (3) and (4) can be equated only under the condition of equal volumes of reaction products and reacting material A. If the volumes are not the same then the Jander equation becomes increasingly invalid as x increases. Both Blum and Li (13) in a study of nickel ferrite formation and Bailey and Russel (14) in a study of spinel formation found that for large values of x the Jander equation did indeed become less valid. Citing the inadequacies given by Carter (12), Bailey and Russel (14) also cited the possibility of deviations due both to limited solubility of B in A at the reaction temperature and to rapid initial reaction rates caused by high initial surface activity combined with changing diffusion rates as the reaction nears completion.

Recent work was done in the area of cordierite formation by Zirczy (15) and by Aza and Espinosa (16). Zirczy (15) studied the formation of cordierite at temperatures between 1250 and 1400°C and times of 2-24 hours from the initial compositions given in Table 1.

Table 2 gives the average particle size for the raw materials as reported by Zirczy (15).

Zirczy (15) concluded that cordierite formed faster in the forsterite-mullite-fused silica body than it did in the spinel-fused silica body.

Table 1. Composition of Cordierite Bodies

Composition	Raw Material	Weight (%)
1	Spinel	48.6
	Fused Silica	51.4
2	Spinel	48.6
	Fused Silica	51.4
	Fused Silica (Excess)	5.0
3	Forsterite	24.1
	Mullite	48.5
	Fused Silica	27.4
4	Composition 1	100.0
	Zircon	5.0
5	Composition 2	100.0
	Zircon	5.0
6	Composition 3	100.0
	Zircon	5.0

Table 2. Raw Material Average Particle Size

Raw Material	Average Particle Size (microns)
Spinel	10
Fused Silica	3
Mullite	25
Fosterite	25
Zircon	2

He also concluded that excess silica was detrimental to cordierite formation from spinel-fused silica, as was the addition of zircon to the compositions at all but the highest temperature studied.

Aza and Espinosa (16) studied the formation of cordierite from kaolin-talc-magnesium carbonate using x-ray diffraction techniques and differential thermal analysis. They concluded that cordierite development occurs in two stages. The first stage involves the formation of cordierite by solid state reaction from protoenstatite mullite, and silica, the reaction starting at 1100°C and reaching a maximum at 1275°C. Above this maximum, the formation of a liquid causes a decrease in the cordierite content, which reaches a minimum at 1335°C. This minimum corresponds to the disappearance of the remaining enstatite. Above 1335°C cordierite again begins to form by crystallization from the liquid phase. Cordierite crystallization continues up to 1375°C and, above that temperature, the cordierite content begins to decrease due to further liquid formation.

CHAPTER III

PROCEDURE

Body Preparation and Firing

Five bodies whose oxide compositions were stoichiometric, or near stoichiometric, cordierite were prepared using as raw materials kaolin, talc, spinel, silica, magnesia, and alumina. Specifications for these materials are presented in Appendix A. These bodies were weighed out in one kg batches according to the weight percentages given in Table 3.

Table 3. Cordierite Body Raw Materials Compositions

Raw Materials	Body No. (Wt %)				
	1	2	3	4	5
Kaolin	65.5	----	----	58.0	----
Talc	34.5	----	----	30.5	----
Spinel	----	48.6	----	11.5	53.6
Silica	----	51.4	51.4	----	51.4
Magnesia	----	----	13.8	----	----
Alumina	----	----	34.8	----	----

All bodies were blended by hand for ten minutes in an enamel container and dry mixed for three hours in one-gallon porcelain ball mills with alumina balls.

Rectangular bars approximately 1/4" x 1/4" x 4" were pressed in a steel die using a Carver laboratory press at 15,000 psi. No binder proved

necessary in any of the bodies. Drying at 300°F for five hours removed any residual moisture.

Five bars of each composition were reacted in an electric furnace which had been preheated to the firing temperature. One bar of each composition was removed at the end of 1, 5, 10, 15, and 20 hours and quenched in air. The bars were fired at temperatures of 1250, 1300, 1350, and 1400°C.

Quantitative Phase Analysis

The quantity of cordierite, mullite, and alumina in the fired bodies was measured using x-ray diffraction techniques. The internal standard technique (17) was chosen as the most accurate because errors due to mass absorption coefficient variations are eliminated.

Internal Standard Theory

The total intensity, I , of x-rays diffracted by the i^{th} component of a uniform mixture of n materials by a plane (hkl) is given by the equation

$$I_i = \frac{K_i f_i}{\mu} \quad (7)$$

where K_i is dependent upon the nature of the component, i , and the geometry of the apparatus, f_i is the volume fraction of the i^{th} component, and μ is the linear absorption coefficient of the powder mixture. If x_i is the weight fraction and ρ_i is the density of the i^{th} component then

$$f_i = \frac{x_i / \rho_i}{\sum_1^n (x_i / \rho_i)} \quad (8)$$

If I is the component whose quantity is to be determined and S is the added internal standard whose amount is known, then

$$I_i = \frac{K_i f_i'}{\mu} \quad \text{and} \quad I_s = \frac{K_s f_s}{\mu} \quad (9)$$

The ratio I_i/I_s is therefore equal to

$$\frac{I_i}{I_s} = \frac{K_i f_i'}{\mu} \frac{\mu}{K_s f_s} \quad (10)$$

Substituting the values for f_i' and f_s from equation (8) yields

$$\frac{I_i}{I_s} = \frac{K_i x_i' \rho_s}{K_s \rho_i x_s} \quad (11)$$

Solving for x_i' yields

$$x_i' = \frac{K_s \rho_i x_s}{K_i \rho_s} \cdot \frac{I_i}{I_s} = K' \frac{I_i}{I_s} \quad (12)$$

as long as x_s is a constant.

If x_i is sought where x_i is the weight fraction in the original sample, then

$$x_i = \frac{x_i'}{1-x_s}$$

and

$$x_i = \frac{K'}{1-x_s} \frac{I_i}{I_s} = k \frac{I_i}{I_s}$$

Therefore, to measure the quantity of any crystalline material in a mixture of other materials, a suitable crystalline internal standard may be mixed with a sample and the weight percent of the material will be proportional to the ratio of the peak intensity of the material and the peak intensity of the standard.

Preparation of Standard Curves

Rutile was chosen as the internal standard because its peaks were well defined and were not super-imposed over those of the other materials in the bodies. The raw materials used to prepare the standard curves were cordierite devitrified from glass, fused α -alumina, and fused mullite. The cordierite glass was devitrified for 32 hours at 1260°C and dry ground in a porcelain mill for three hours and screened to -325 mesh. This method of preparing cordierite for the standards was chosen because it produced cordierite with no detectable crystalline impurity. The α -alumina and mullite were sieved to -325 mesh. All standard materials were analyzed by x-ray diffraction for detection of impurities. No crystalline impurities were found with the exception of a trace of alumina in the mullite.

A series of cordierite, alumina, mullite standard compositions was prepared containing the percentages shown in Table 4. The bodies were blended for 36 hours in polyethylene jars, using porcelain balls as a blending media. Three 3-gram samples ($3.0000 \pm .0005$) were taken from each standard body and each blended with one gram ($1.0000 \pm .0005$) of rutile to prepare the samples for x-ray diffraction analysis. Blending was accomplished by placing the sample and the rutile in a plastic cylinder with two glass marbles and mechanically shaking for one hour.

Table 4. Standard Body Compositions

Cordierite (Wt %)	Mullite (Wt %)	Alumina (Wt %)
30	35	35
40	30	30
50	25	25
60	20	20
70	15	15
80	10	10
90	5	5

Unencumbered diffraction peaks were selected for determining the content of each phase and scan limits were set for each peak at background intensities (see Table 5). These peaks were selected as the ones most free of interference and reasonably close to the rutile peak.

Table 5. X-Ray Peak Locations

Phase	Approximate Peak Position (°2θ)	Scan Limits (°2θ)
Mullite	16.5	16.00 - 16.75
Rutile	27.5	27.00 - 28.00
Cordierite	29.5	29.00 - 30.00
Alumina	37.8	37.40 - 38.15

One x-ray powder pack was prepared for each of the three samples taken from each standard composition. Powder packs were prepared in

Phillips rectangular sample holders using the method described by McCreery (17) with the exception that the powder was packed against a frosted glass slide surface rather than a flat glass surface. The powder packs were scanned at $1/4^\circ 2\theta$ using a Phillips diffractometer under the conditions given in the Appendix. The integrated intensities for the peaks were measured by summing the counts between the $^\circ 2\theta$ scan limits given in Table 5 for each peak. The background intensities were determined by summing the counts for 30 seconds at the lower scan limit and 30 seconds at the upper scan limit and multiplying the total by the factor necessary to make the total count time at the scan limits equal to the time required to scan the peak between the limits. The peak intensities were found by subtracting the background from the integrated peak intensities. The intensities of the mullite, cordierite, and alumina peaks were each divided by the intensity of the rutile peak and plots were made of intensity ratio versus weight percent for each of the three materials. Linear regression analysis was used to determine the best straight line fit for the data points in each plot. These standard curves are shown in Figures 3, 4, and 5.

Quantitative Phase Analysis of Unknowns

Each fired sample was crushed in a steel die. The resulting lumps were reduced by hand to a coarse powder using a porcelain mortar and pestle. This powder was placed in a Fisher automatic mortar and pestle and ground to -325 mesh.

Three grams ($3.0000 \pm .0005$) of each sample were mixed with one gram ($1.0000 \pm .0005$) of rutile in a plastic cylinder and blended in the

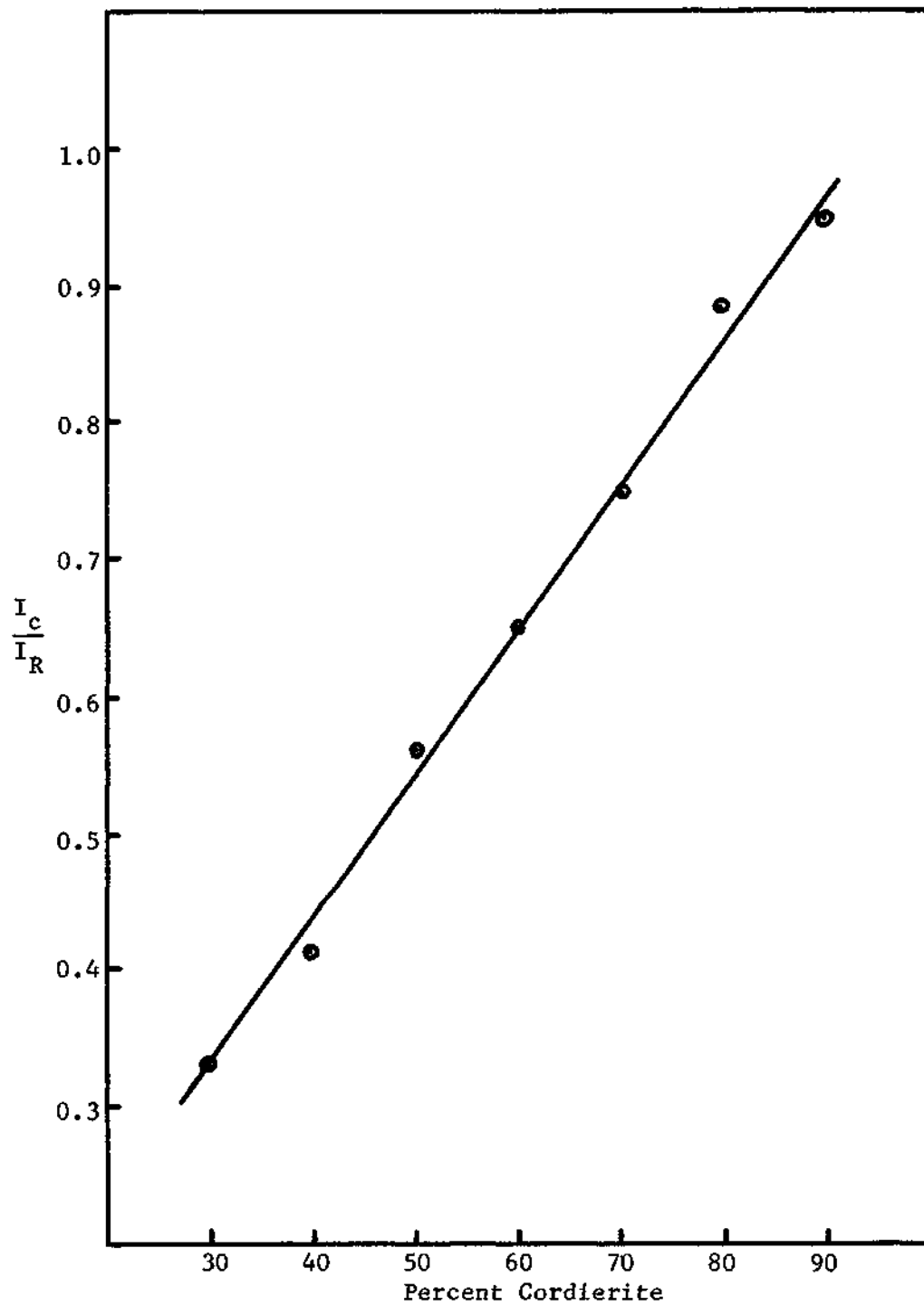


Figure 3. Cordierite Calibration Curve (29.5° Peak)

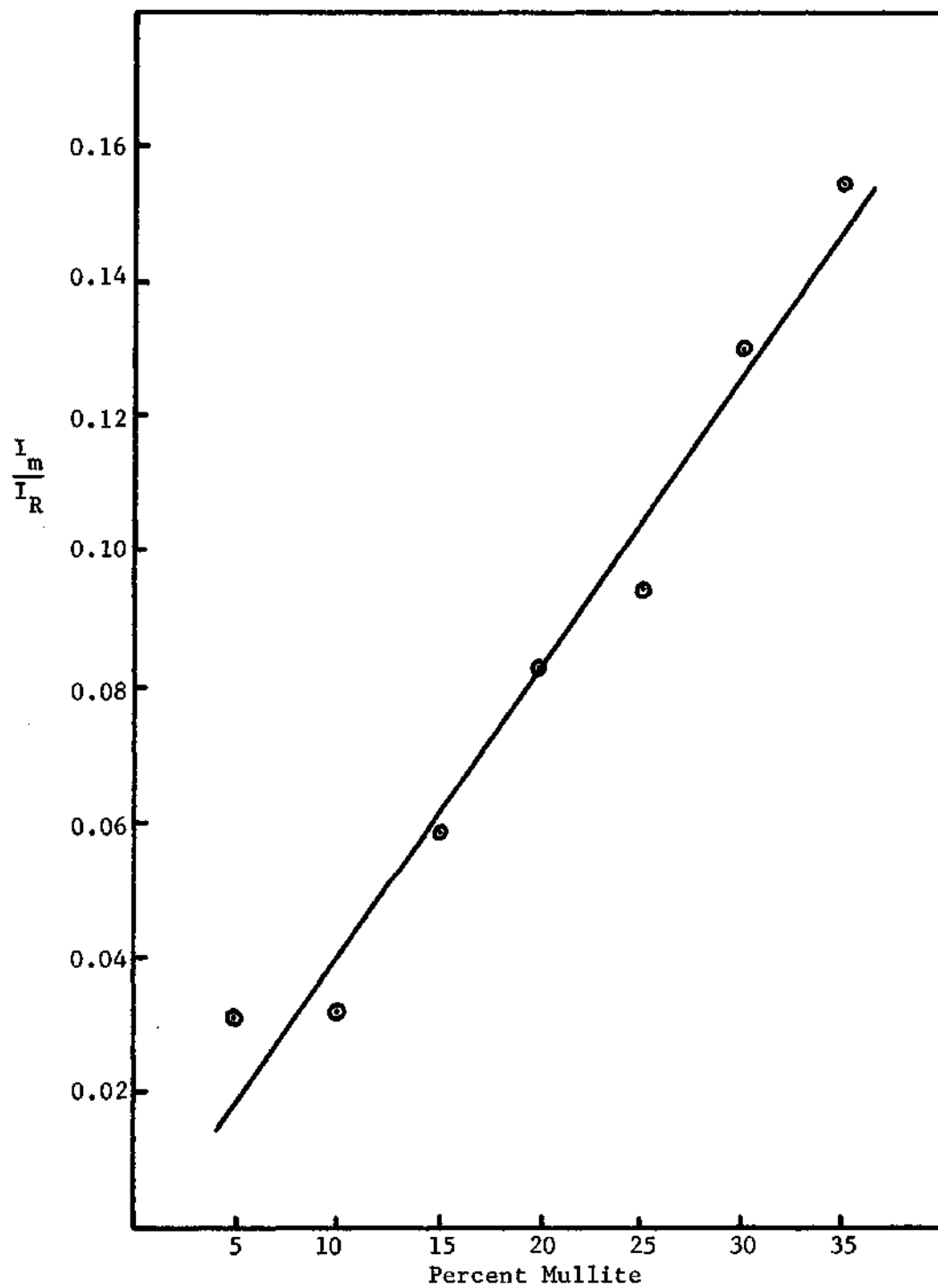


Figure 4. Mullite Calibration Curve

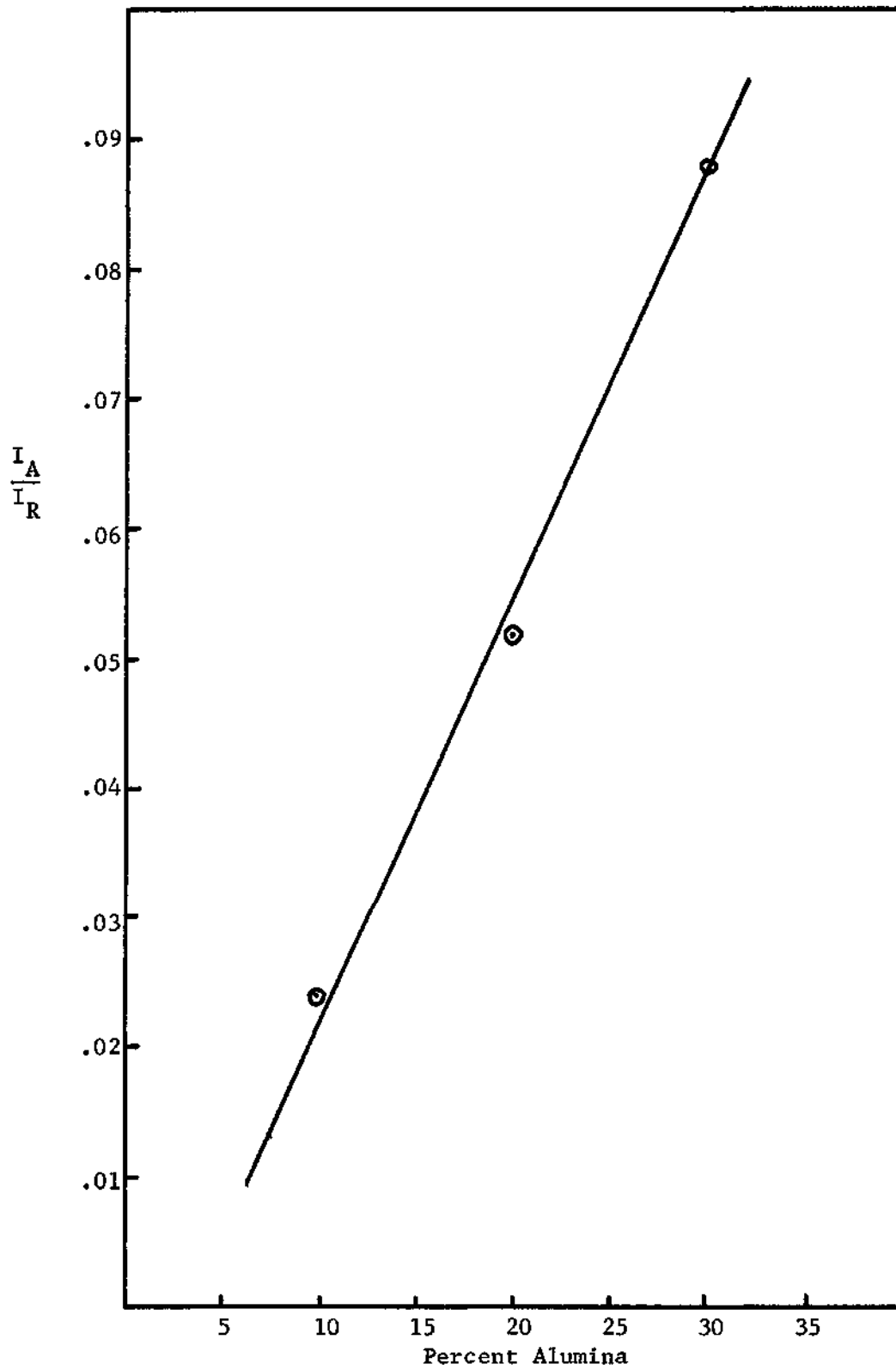


Figure 5. Corrected Alumina Calibration Curve

same manner as the standards. Two powder packs were prepared from each sample. Quantitative x-ray analysis was performed on the powder packs using the same procedure that was used on the standards. The kaolin-talc, kaolin-talc-spinel, spinel-silica, and spinel-silica-excess spinel samples were scanned for mullite and cordierite. The alumina-silica-magnesia samples were scanned for mullite, cordierite, and alumina. The peak intensity ratios were determined and the weight percent of the materials determined from the standard plots. Two determinations were made for each material in each sample and the average reported.

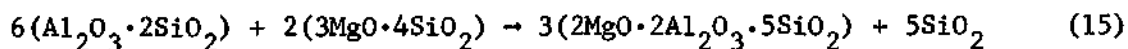
The kaolin-talc and kaolin-talc-spinel samples were also scanned from $5-75^{\circ} 2\theta$ to determine if enstatite was present.

CHAPTER IV

RESULTS AND DISCUSSION

Reaction of Kaolin and Talc

Kaolin and talc when reacted to form cordierite will produce an excess of SiO_2 if compounded according to:



If the reaction goes to completion a body containing 85.4 weight percent cordierite could be obtained. The results of x-ray analysis of the various samples of the kaolin-talc body (composition 1, equation (15)) show that this reaction was far from complete at the times and temperatures studied. The weight percent cordierite as determined by x-ray analysis, Table 6, shows that large amounts of cordierite formed during the first hour. The cordierite content was found to increase with temperature during the early hours between 1250 and 1350°C. The cordierite content also appeared to increase with time at 1250°C, but at 1300°C and 1350°C the cordierite remained essentially the same at twenty hours as it was at one hour. At 1400°C a significant decrease was noted in the cordierite content. The cordierite content at one hour was 30 percent lower than that of the 1350°C sample and was 15 percent below that of the 1250°C sample. While cordierite content did increase with time at 1400°C, it reached a level at 20 hours equal only to that of the 1250°C sample at one hour.

Table 6. Cordierite Weight Percent in Kaolin-Talc Body
(Composition 1)

Temperature (°C)	Time (hr)				
	1	5	10	15	20
1250	52.0*	50.5	59.0	63.5	66.0
1300	56.0	63.0	69.0	59.0	63.5
1350	65.0	67.5	58.0	61.0	66.0
1400	35.0	45.0	40.0	49.0	52.5

* Problems encountered with the x-ray equipment make this value disputable.

Examination of x-ray patterns for the kaolin-talc samples at one hour revealed the presence of peaks due to enstatite at 1250, 1300, and 1350°C with the apparent intensities decreasing with increased firing temperature. At 1400°C no major peaks associated with enstatite were present; however, a large amorphous hump commonly associated with the presence of a glassy phase was noted.

Closer examination of Figure 6, which shows the cordierite content of the kaolin-talc samples plotted versus time for the four temperatures studied, reveals a trend that occurs in the three higher temperature samples. The cordierite content appears to increase with time at first, followed by a drop in cordierite at longer times, and then another increase. In light of the work done by Aza and Espinosa (16), this result could be explained in terms of (1) an initial period in which the formation of cordierite by solid state reaction is the dominant factor, followed by (2) a period in which the dominant factor is the increase of the liquid phase at the expense of primarily crystalline cordierite, and (3) another

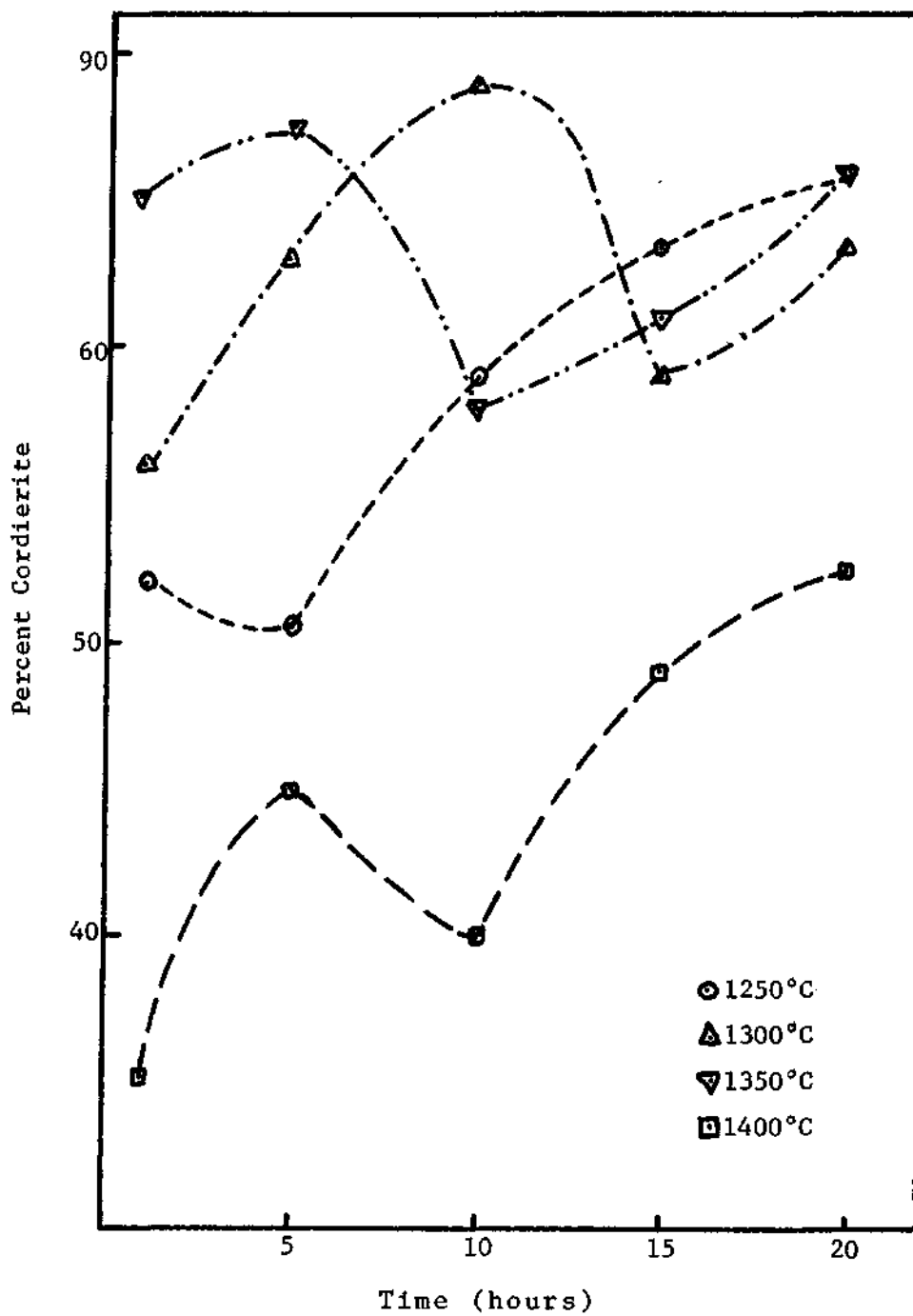


Figure 6. Effect of Time and Temperature on Cordierite Content of Kaolin-Talc Body (Composition 1)

period of cordierite growth, this time by means of the crystallization of cordierite from the liquid phase.

If this explanation is correct, it would be expected that as temperature increased the time at which the above three reaction regions dominate would decrease. Examination of the curves for 1300 and 1350°C reveal that the observed maximum and minimum cordierite content points do occur at an earlier time in the the 1350°C sample. The lack of cordierite formation in the 1400°C samples would also come as no surprise. Since the temperature is above the temperature at which the first liquid could be expected to form by localized melting (1355°C), the formation of the liquid phase would start sooner and proceed more rapidly than at lower temperatures, where the formation of a liquid phase is probably due to the presence of impurities. Thus at 1400°C, the extremely rapid glass formation significantly retarded the formation of the initial cordierite by solid state reaction that had been observed at lower temperatures.

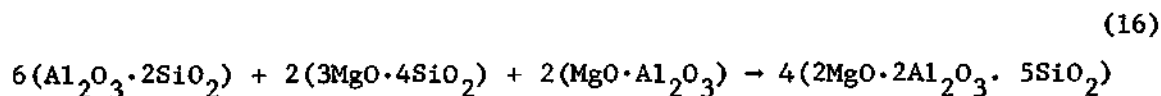
Previous authors (10) have stated that the presence of mullite was a key factor in the formation of cordierite and that cordierite formed rapidly when significant mullite was present and very slowly when mullite was not present in significant amounts. Analysis of the mullite content of the kaolin-talc body, Table 7, shows that at all times and temperatures significant amounts of mullite, 15 ± 3 percent, were present and that no rapid cordierite increase took place consuming the available mullite. Thus, the mullite presence did not appear to either enhance or retard cordierite formation.

Table 7. Mullite Weight Percent in Kaolin-Talc Body
(Composition 1)

Temperature (°C)	Time (hr)				
	1	5	10	15	20
1250	17.0	16.0	16.5	15.0	15.0
1300	18.0	16.0	14.5	14.0	12.5
1350	15.0	15.0	14.5	14.0	14.0
1400	16.5	16.5	15.5	15.0	15.5

Effects of Spinel Additions

Equation (15) shows that a complete reaction of kaolin and talc to form cordierite yields excess silica. By the addition of sufficient spinel this reaction can be changed to yield only cordierite with no silica excess, the reaction being



Analysis of the cordierite content in this body, Table 8, shows that the addition of the spinel to composition 1 did cause a small increase in the cordierite content between 1250 and 1350°C when compared with the corresponding samples of composition 1, Table 6. Examination of the cordierite content at 1400°C, however, reveals a significant change from that observed in composition 1 at the same temperature. While the drop in cordierite content at 1400°C that occurred in composition 1 was also observed to occur in composition 4, it was not nearly as significant as can be seen in Figure 7 which shows the cordierite content at 1350 and

1400°C in composition 1 and the cordierite content at 1400°C in composition 4.

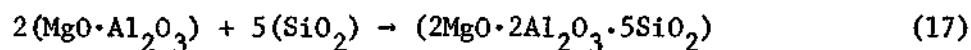
Table 8. Cordierite Weight Percent in Kaolin-Talc-Spinel Body (Composition 4)

Temperature (°C)	Time (hr)				
	1	5	10	15	20
1250	59.0	63.0	70.0	70.0	72.0
1300	63.0	63.0	71.0	68.5	74.0
1350	64.0	69.0	67.0	67.0	69.5
1400	59.5	59.0	58.0	71.0	73.0

Examination of Figure 8, which shows cordierite content from Table 8 plotted versus time, reveals the same sequence of cordierite formation occurring as was observed in the kaolin-talc body, but at a reduced magnitude. Spinel entering the reaction delayed and reduced the formation of the liquid even above the 1355°C point at which the first liquid might be expected. However, due to impurities promoting lower glass formation temperatures, the cordierite content was much lower than theoretically possible.

Reaction of Spinel-Silica

Cordierite can also be formed by the reaction of spinel and silica, the reaction being



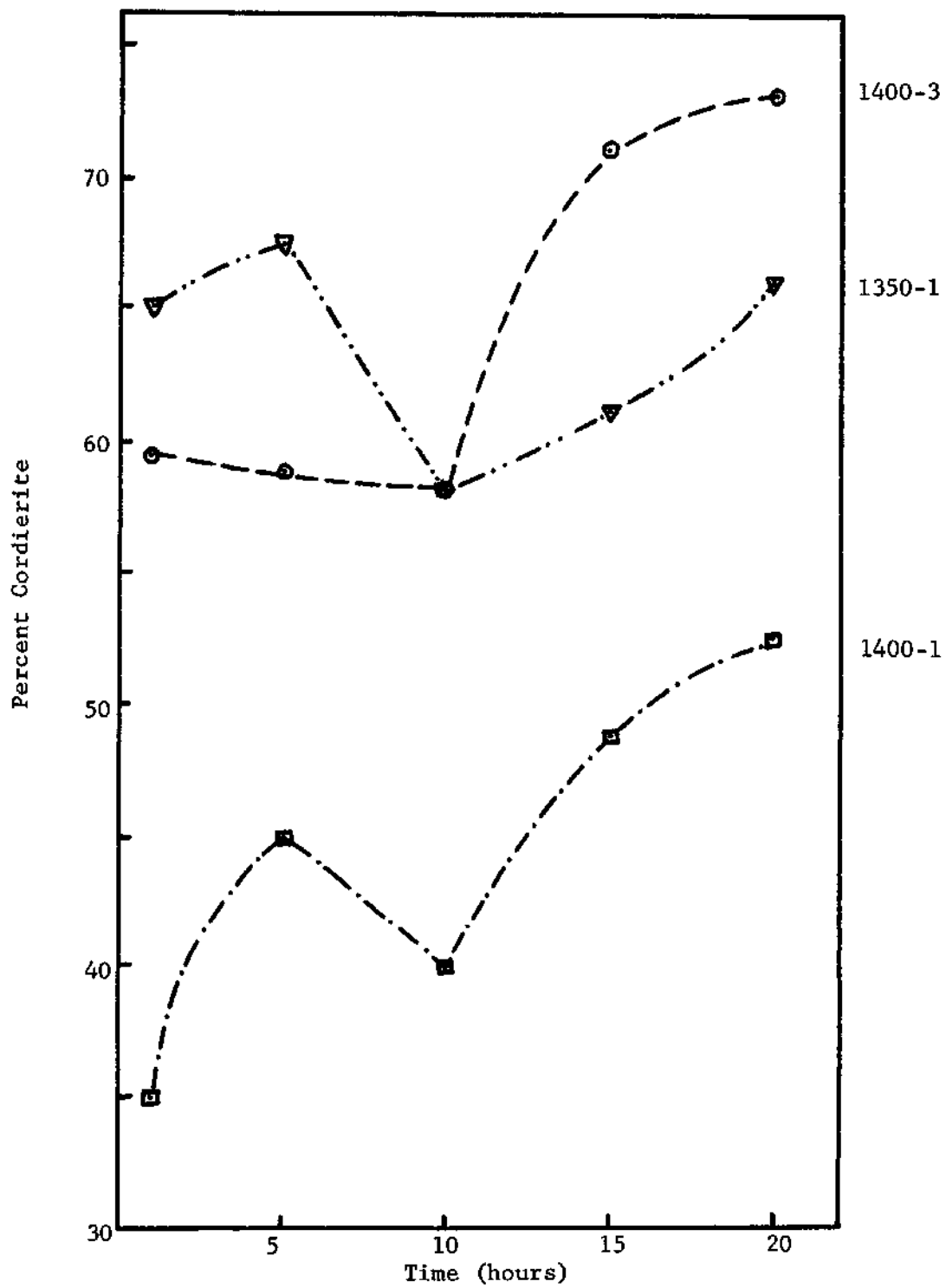


Figure 7. Effect of Time on Cordierite Content of Kaolin-Talc Body (Composition 1) at 1350°C and 1400°C and Kaolin-Talc-Spinel Body (Composition 4) at 1400°C

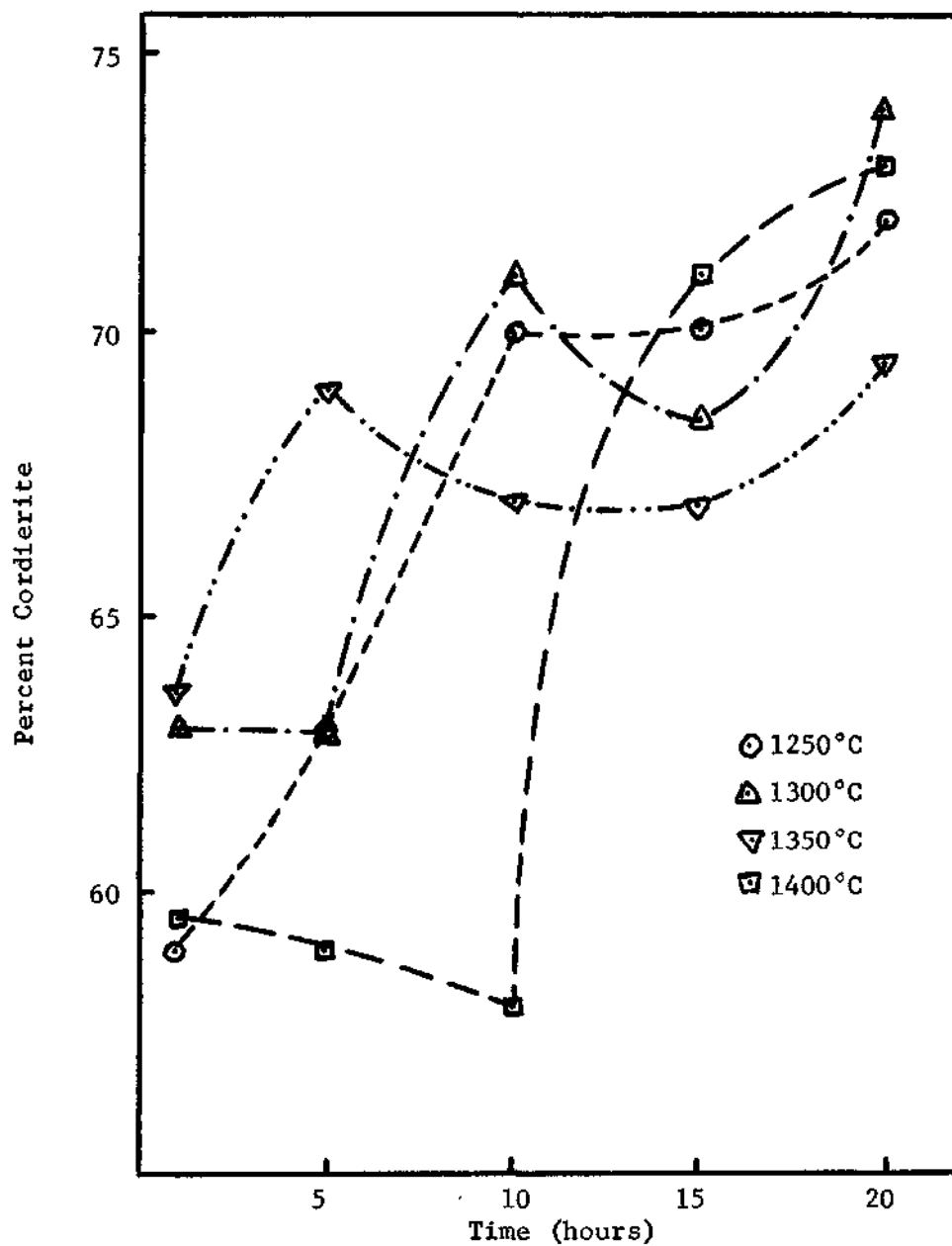


Figure 8. Effect of Time and Temperature on Cordierite Content of Kaolin-Talc-Spinel Body (Composition 4)

Analysis of the cordierite content of composition 2, Table 9, shows the same fast initial reaction during the first hour followed by a gradual increase with time (Figure 9) as was observed in the kaolin-talc body. It was also observed that while the increase in cordierite content between 1250 and 1300°C was only 10 to 15 percent and that that from 1350 to 1400°C was less than five percent, the increase between 1300 and 1350°C was quite large. The cordierite content increased nearly 30 percent during the first hour, the difference dropping to 20 percent at longer times.

Table 9. Cordierite Weight Percent in Spinel-Silica Body (Composition 2)

Temperature (°C)	Time (hr)				
	1	5	10	15	20
1250	29.0	37.0	44.0	45.0	45.0
1300	37.0	53.0	54.0	57.0	59.0
1350	65.0	----	76.5	81.5	77.0
1400	69.5	76.0	79.0	80.0	90.0

Since the cordierite content in this body increased continuously with time and temperature, unlike that in the kaolin-talc body, it appears that the cordierite is formed by solid state reaction alone.

Examination of the spinel-silica body for the presence of mullite failed to detect any at any time or temperature, showing that mullite is not necessary for cordierite formation.

Comparison with Kaolin-Talc and Kaolin-Talc-Spinel

At 1250°C the spinel-silica body did not compare favorably with the kaolin-talc and kaolin-talc-spinel bodies as can be seen in Figure 10.

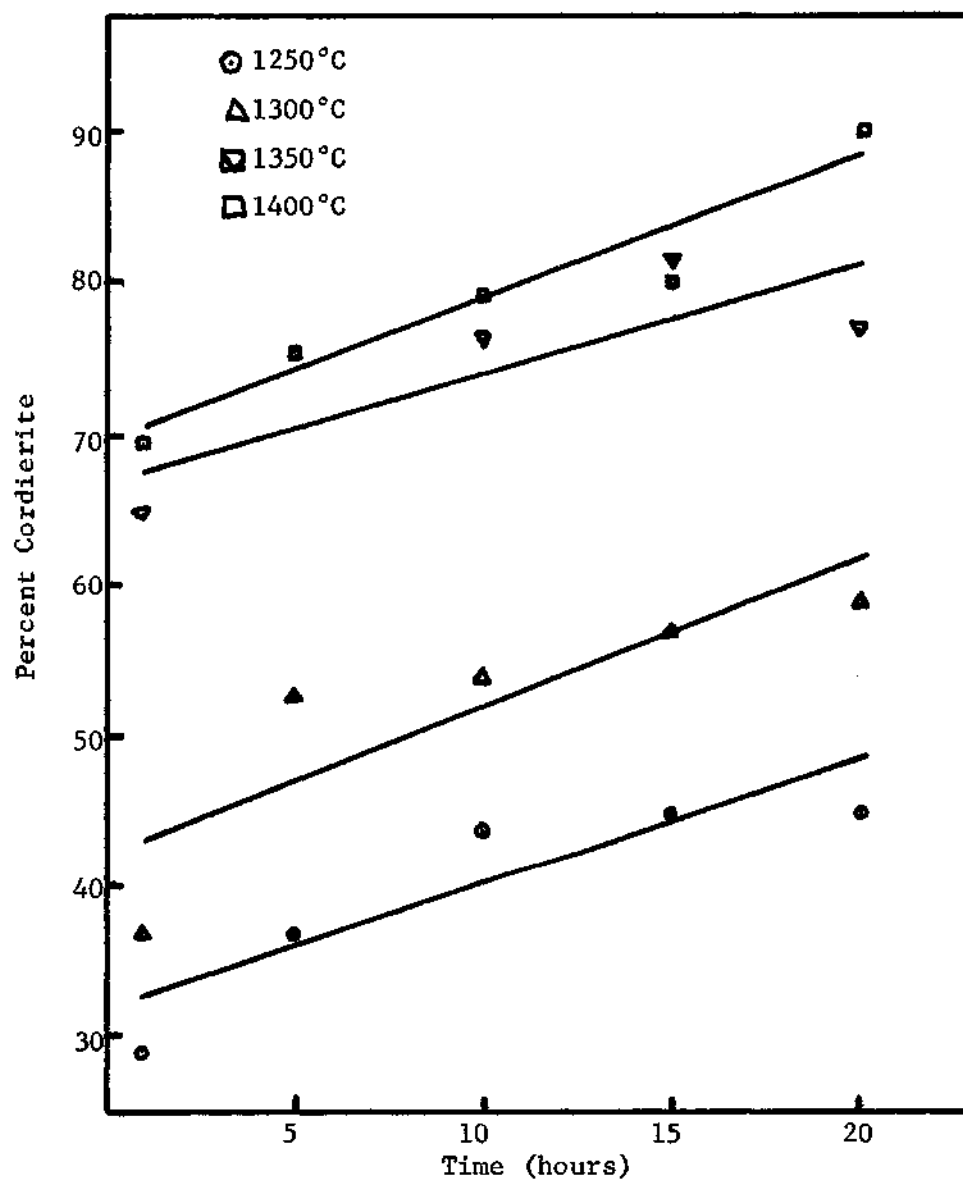


Figure 9. Effect of Time and Temperature on Cordierite Content of Spinel-Silica Body (Composition 2)

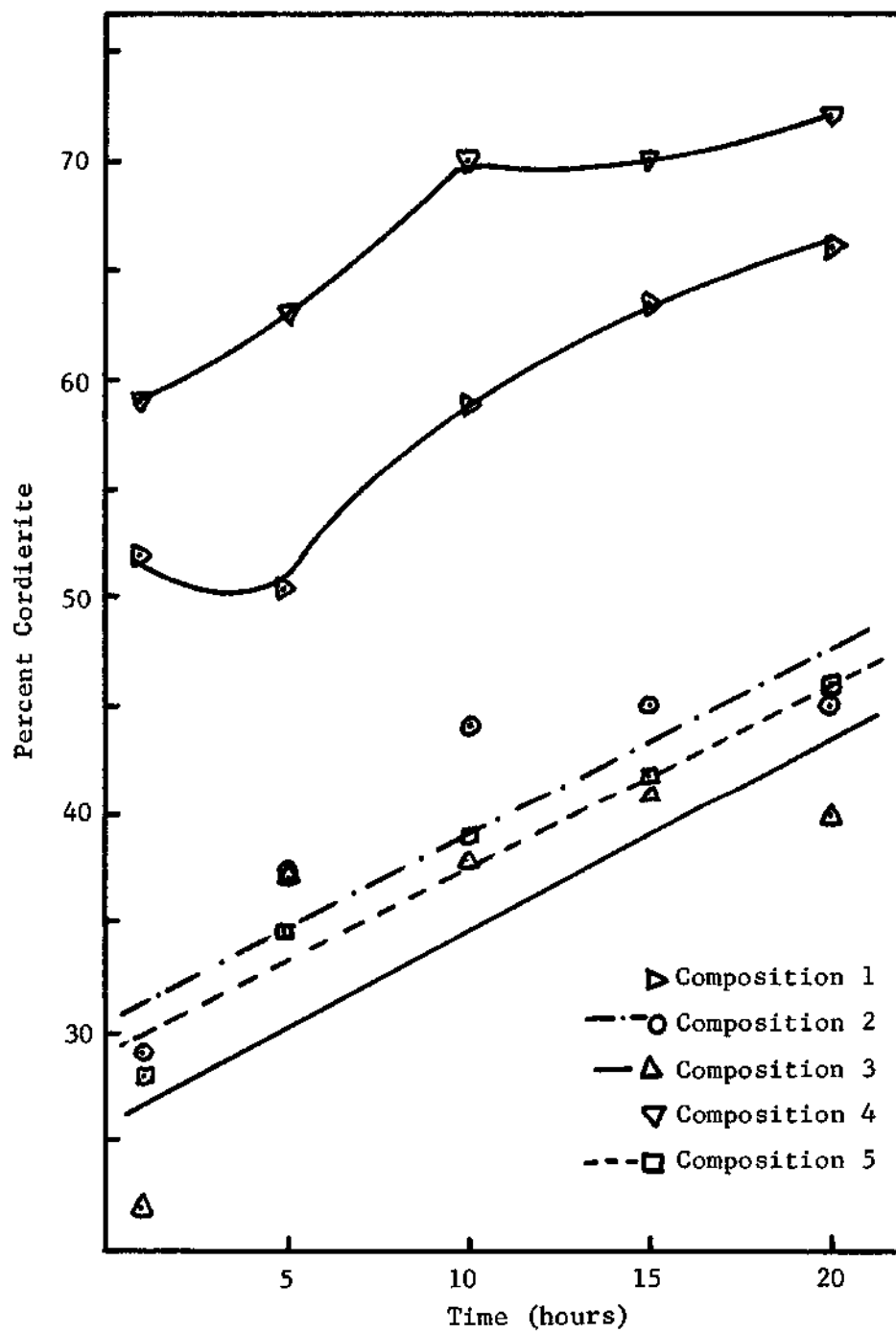


Figure 10. Effect of Time on Cordierite Formation from Various Initial Raw Material Compositions at 1250°C

The cordierite content was approximately one-half that of bodies 1 and 4 at one hour and this ratio did not change with time. Figure 11 shows that at 1300°C the content was still approximately one-half of bodies 1 and 4 during the early hours, but the difference decreased with time, being less than 15 percent at 20 hours as opposed to nearly 30 percent at one hour. Above 1300°C (Figures 12 and 13) the situation was reversed. The spinel-silica body contained more cordierite than did bodies 1 and 4 and at 1400°C it was double that of the kaolin-talc and one and one-half times that of the kaolin-talc-spinel, having suffered no deterioration as did bodies 1 and 4.

A comparison of cordierite formation between the spinel-silica body and the kaolin-talc body would not be complete without mentioning particle size. Appendix A gives the particle size for the raw materials used. It can be seen that both the spinel and the silica are of smaller particle size than the kaolin and the talc, particularly the silica which is three orders of magnitude smaller. This would mean that there is more surface area available for reaction in the spinel-silica body than in the clay-talc body.

Since the kaolin and talc reacted to form cordierite faster than the spinel and silica at the lower temperatures, it appears the starting composition is more important than the particle size. Formation from kaolin and talc involves the reaction of enstatite, mullite, and silica. These three materials form a triangle in the alumina-magnesia-silica phase diagram which includes the cordierite primary phase field and the lower eutectic temperatures. However, spinel and silica are on the same side at the lower eutectic compositions and any reaction between the two

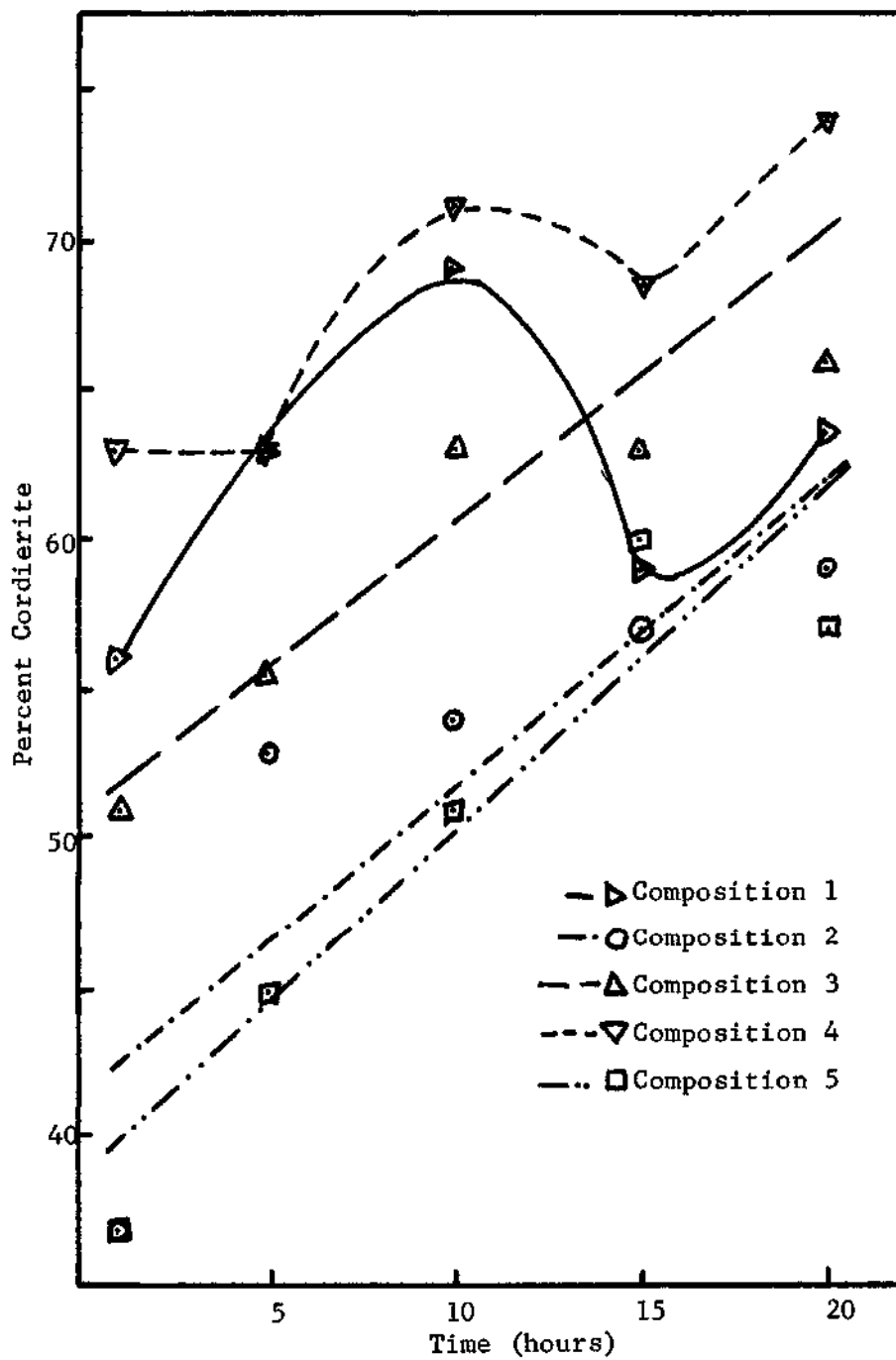


Figure 11. Effects of Time on Cordierite Formation from Various Initial Raw Materials at 1300°C

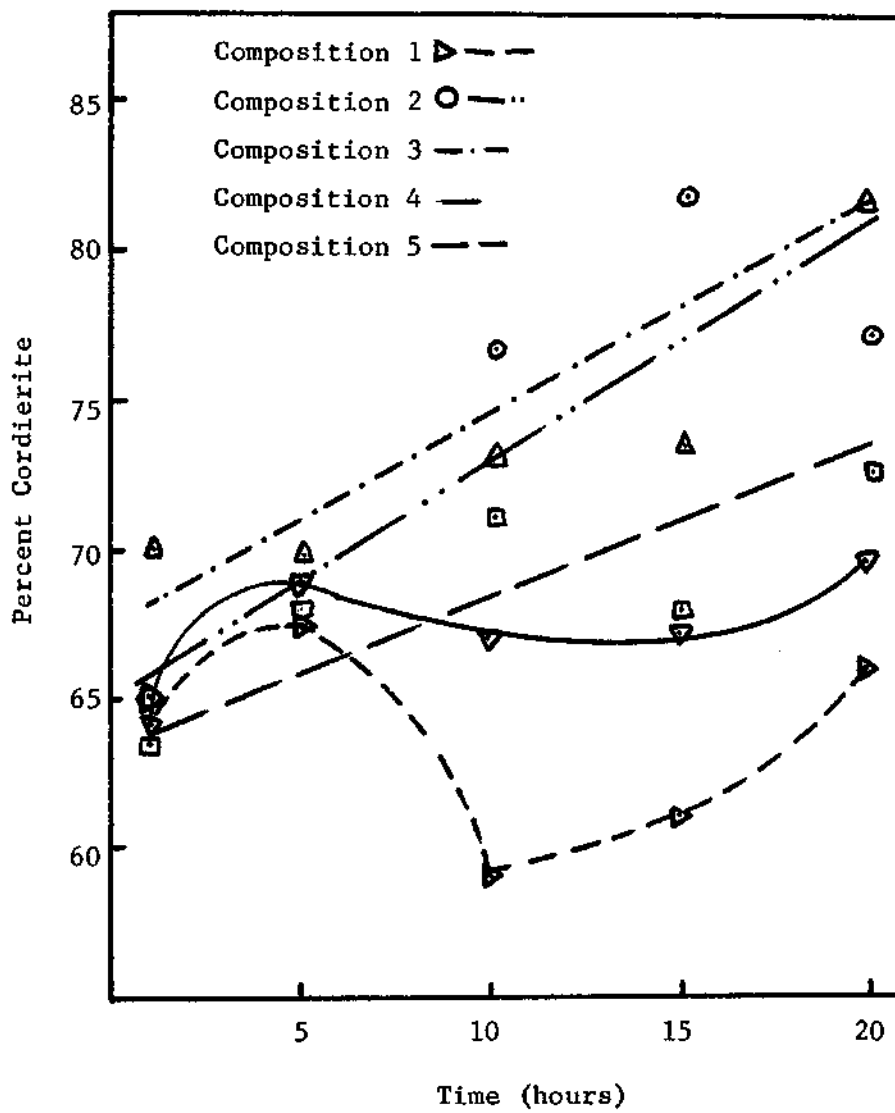


Figure 12. Effects of Time on Cordierite Formation from Various Initial Raw Materials Compositions at 1350°C

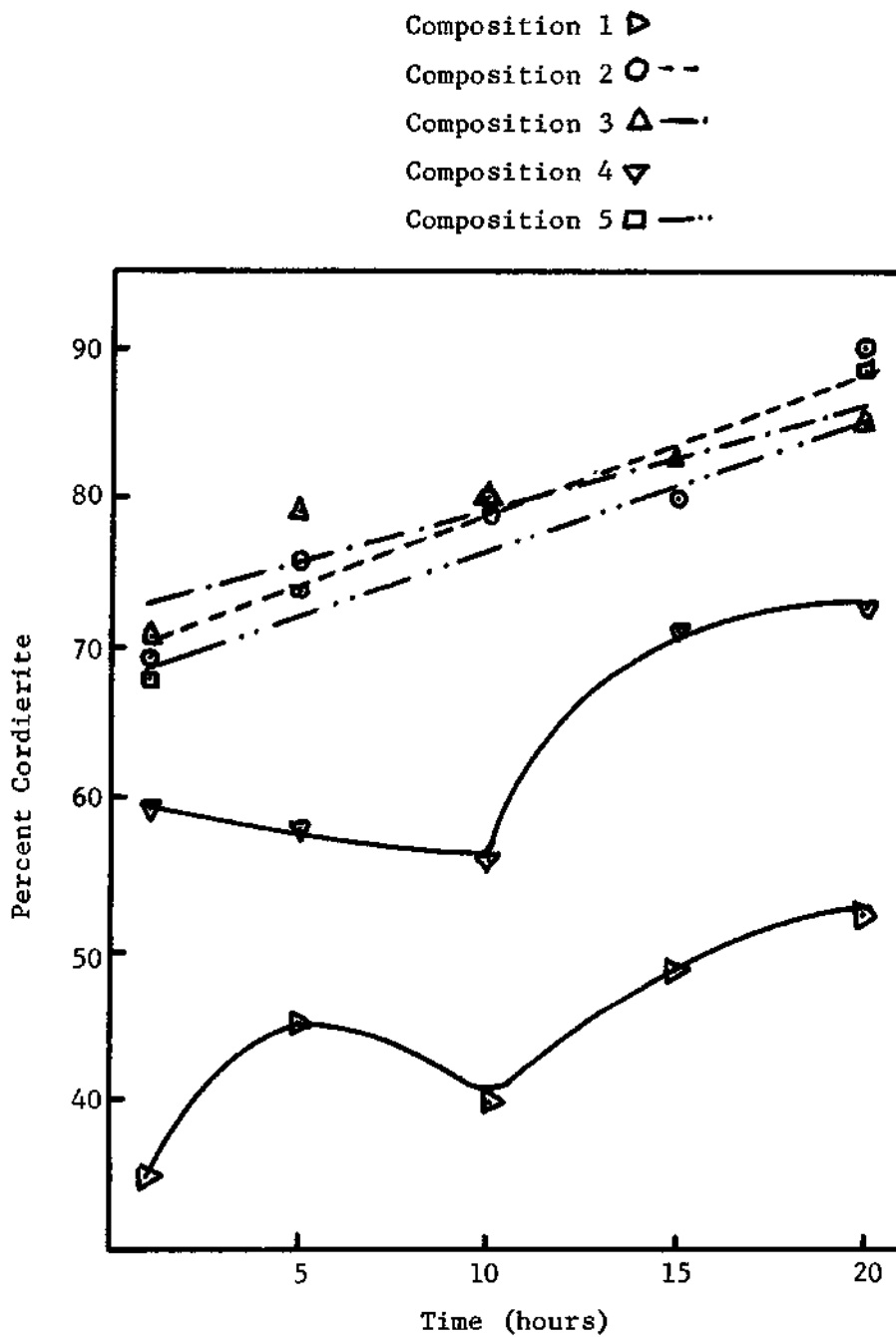


Figure 13. Effects of Time on Cordierite Formation from Various Initial Raw Material Compositions at 1400°C

would be expected to fall along a line between them. This line passes through the spinel, mullite, and silica primary phase field and is on the high temperature side of the 1440 to 1455°C eutectics.

Effects of Spinel Addition

In order to determine if increasing the concentration of the spinel relative to that of silica would enhance the formation of cordierite, spinel was added to body 2 in the amount of five weight percent of the weight percent of body 2.

Analysis of the cordierite content of this body, given in Table 10, and shown in Figure 14, failed to reveal any significant differences in cordierite content with the exception of the fact that the cordierite content was slightly lower in the spinel-silica-excess spinel than it was in the spinel-silica body. The difference is most likely due not to a decrease in the amount of cordierite forming, but to a reduction of its concentration in the body by the excess spinel.

Table 10. Cordierite Weight Percent in Spinel-Silica-Excess Spinel (Composition 5)

Temperature (°C)	Time (hr)				
	1	5	10	15	20
1250	28.0	34.5	39.0	42.0	46.0
1300	37.0	45.0	51.0	60.0	57.0
1350	63.5	68.0	71.0	68.0	72.5
1400	68.0	74.0	80.0	----	88.5

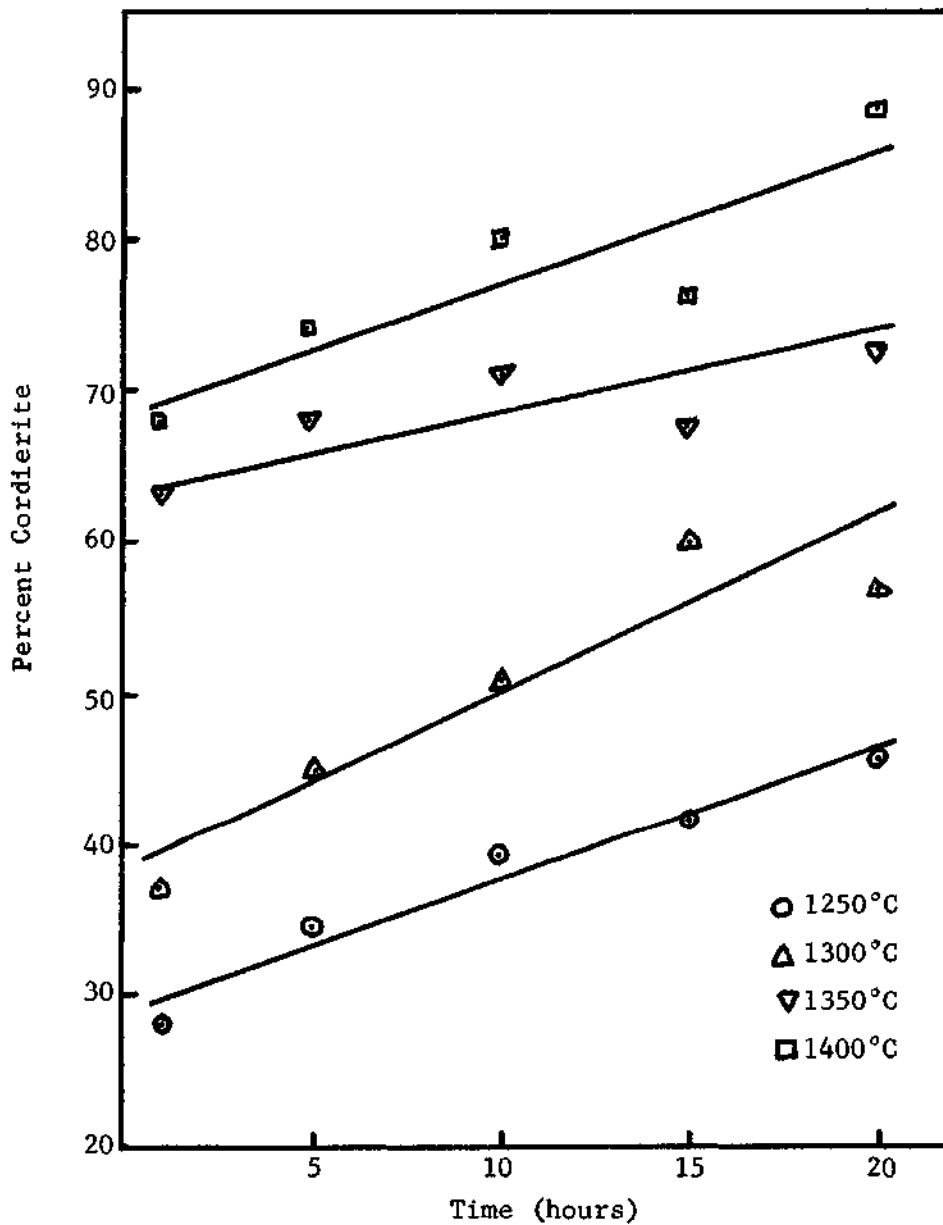
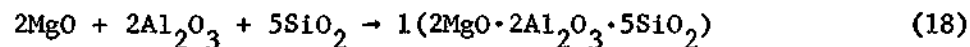


Figure 14. Effect of Time and Temperature on Cordierite Content of Spinel-Silica-Excess Spinel Body (Composition 5)

Reaction of Alumina-Magnesia-Silica

The three primary oxides of cordierite were reacted to form cordierite.



The reaction results as determined by x-ray analysis are given in Table 11.

Table 11. Cordierite Weight Percent in Alumina-Silica-Magnesia (Composition 3)

Temperature (°C)	Time (hr)				
	1	2	3	4	5
1250	22.0	37.0	38.0	41.0	40.0
1300	51.0	55.5	63.0	63.0	66.0
1350	70.0	70.0	73.0	73.5	81.5
1400	71.0	79.0	80.0	83.0	85.0

They show that, as with previous bodies, a fast reaction took place during the first hour, followed by a slow increase with time. This is evident in Figure 15. A large increase in cordierite content was noted between 1250 and 1300°C, the content at 1300°C being more than double that at 1250°C. This difference of between 25 and 30 percent was maintained with time. The increase between 1300 and 1350°C was about half that occurring between 1250 and 1300°C, and the increase between 1350 and 1400°C was even smaller, being less than five percent at 20 hours.

It appears that the formation of cordierite from the three primary oxides is one of solid state reaction.

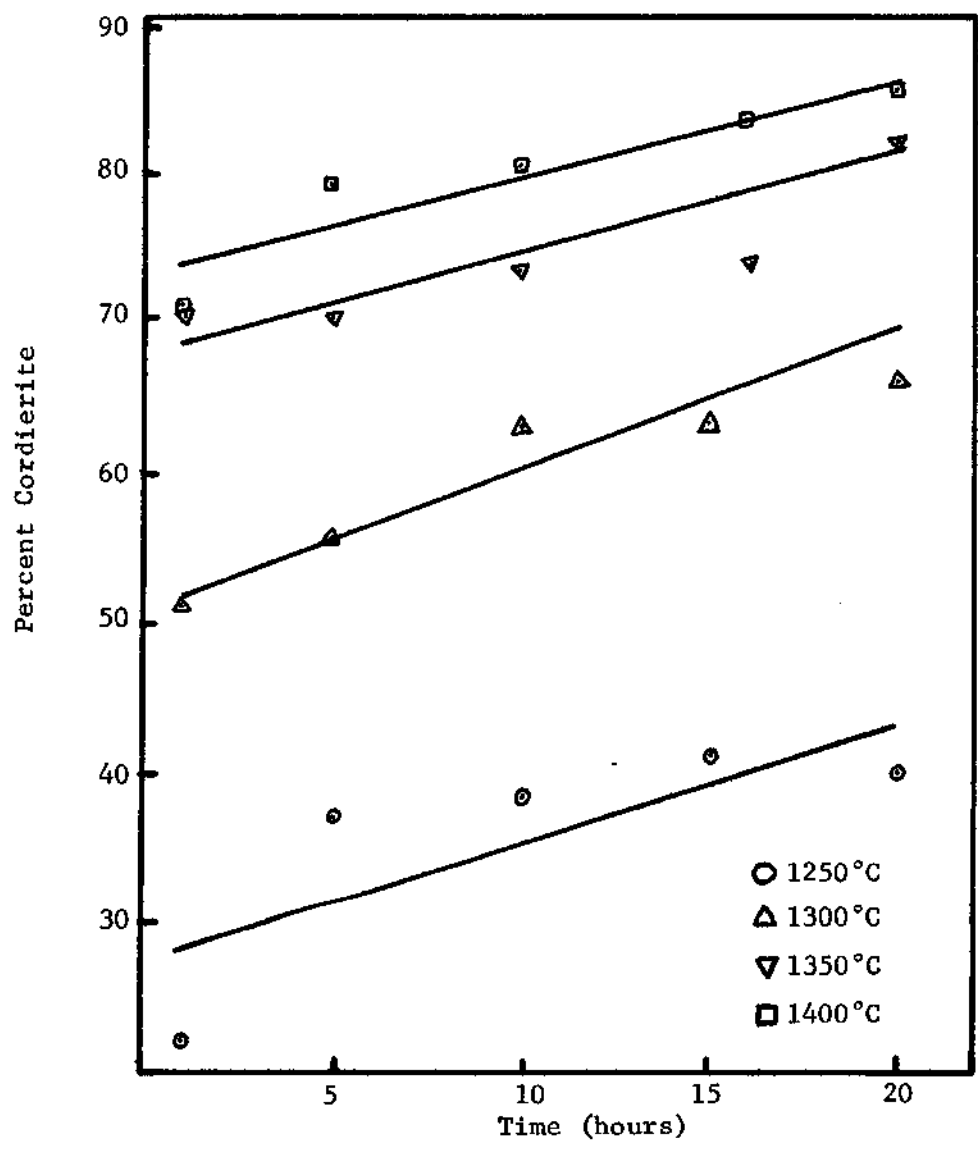


Figure 15. Effect of Time and Temperature on Cordierite Content of Alumina-Magnesia-Silica Body (Composition 3)

Examination of the body for crystalline alumina or mullite failed to detect either at any time or temperature.

Comparison with Spinel-Silica

At 1250°C the spinel-silica body appeared to form slightly more cordierite; but, at 1300°C the silica-alumina-magnesia body appeared to form more. The differences in cordierite content were not large, generally being less than 10 percent, however, and at higher temperatures they were even smaller. Since the particle sizes of the spinel, magnesia, and alumina were very close, it appears that neither spinel nor the primary oxides possess an advantage over the other when reacted with silica to form cordierite.

Reaction Kinetics

Analysis of reaction kinetics by traditional methods for the kaolin-talc bodies (Compositions 1 and 4) was impossible due to the reaction to form cordierite being controlled by four mechanisms, each with different reaction rate constants. These four mechanisms in sequential order were (1) surface reaction, (2) solid-state diffusion, (3) liquid formation, and (4) nucleation - crystallization from the liquid.

Reaction kinetics were less complicated in the silica-spinel, silica-spinel-excess spinel, and magnesia-alumina-silica compositions due to a lack of significant liquid formation. Thus reaction kinetics were controlled by initial surface reaction and later by solid-state diffusion reaction. The Jander model of reaction kinetics as described in the Survey of Literature was applied to these compositions and the values of $K_J t$ found, and from them the values of K_J determined. The natural log of the K_J values was plotted versus $1/T^\circ K$ for each composition (Figure 16)

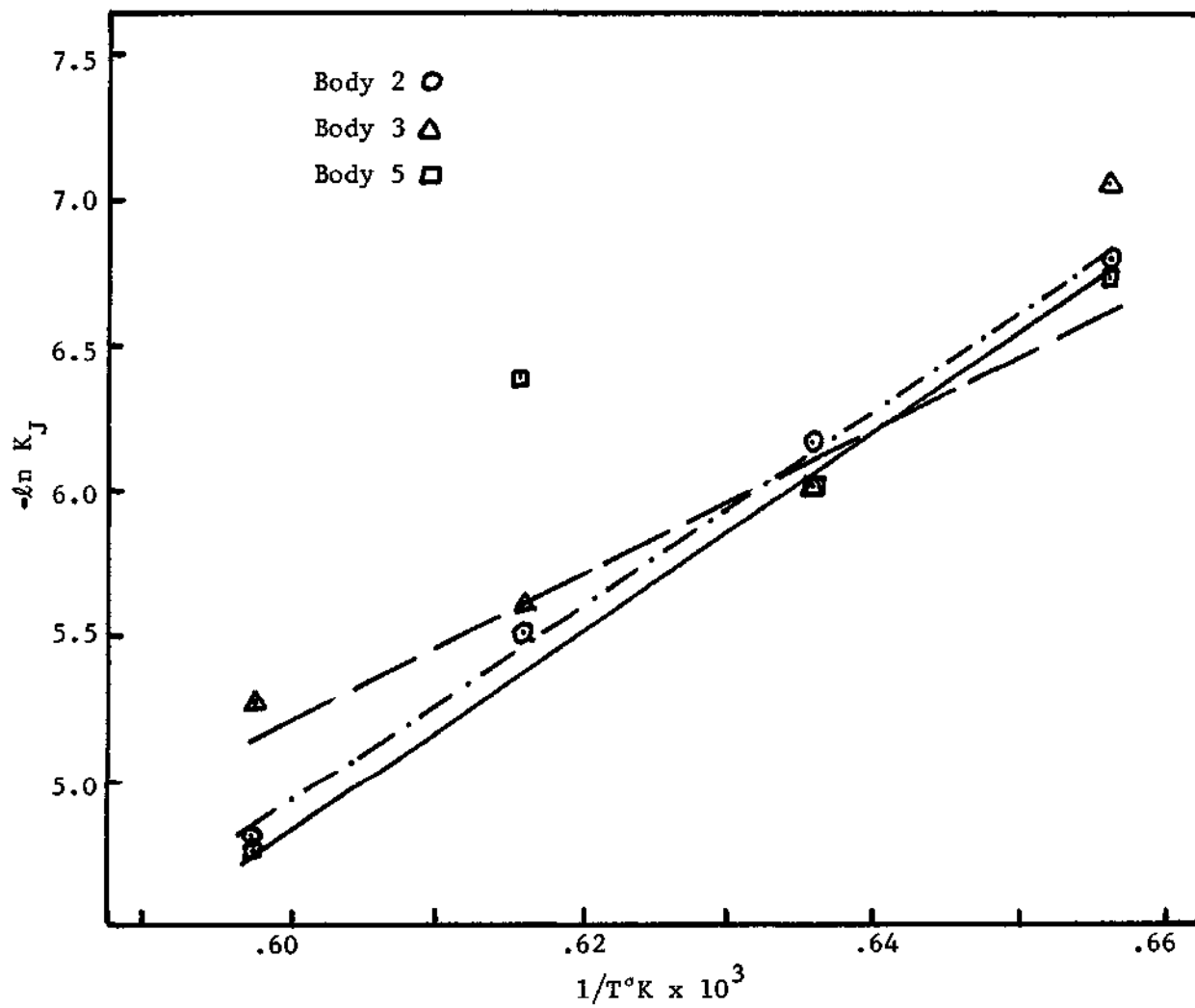


Figure 16. $-\text{Log } K_J$ versus $1/T^{\circ}K$ for Bodies 2, 3, and 5

and the activation energies calculated (Table 12).

Table 12. Jander Activation Energy

Body No.	Activation Energy Kcal/mole
2	67
3	59
5	56

The activation energies calculated were all close together, but somewhat lower than activation energies reported by other investigators such as Bailey (14) who gave a value of 90.5 Kcal/mole for the formation of spinel and Bronson (18) who gave a value of 77 Kcal/mole for the formation of zinc spinel.

It must be considered that the application of the Jander model to the results given here in order to determine activation energies may be erroneous. Previous authors, Bailey (14) for example, have shown that the Jander model cannot be readily applied to cases where high reaction product contents are present. From results of this study it can be seen that large amounts of reaction products were present even at one hour due to the large quantity of cordierite formed by surface reaction. As stated by previous authors, kinetic theory at present is insufficient to describe the time-temperature relationship for reactions involving high surface area reactants where the majority of the product formed is by surface reaction and not by bulk diffusion.

CHAPTER V

CONCLUSIONS AND RECOMMENDATIONS

Conclusions

1. For all compositions and temperatures, the majority of cordierite formed in the first hour of firing due to the high surface area of the reactants and after the first hour of firing cordierite content increased gradually with time.
2. The formation of cordierite with time below 1400°C in the kaolin-talc and kaolin-talc-spinel bodies was complex, apparently involving initial solid state reaction which increased cordierite content, subsequent liquid formation dissolving already formed cordierite, and later increased cordierite content due to crystallization from the liquid.
3. At 1400°C deterioration was observed in the cordierite content of both the kaolin-talc and kaolin-talc-spinel bodies due to the liquid formation which essentially eliminated the solid state reaction observed at lower temperatures. The cordierite content still tended to increase with time; but the content was less than that found at all lower temperatures.
4. The addition of spinel to the kaolin-talc body caused an increase in the cordierite content over that in the kaolin-talc body by moving the composition to stoichiometric cordierite. The resulting decreased liquid formation caused by the spinel addition reduced the deterioration in the cordierite which occurred in the kaolin-talc body at 1400°C.

5. No significant change with time was found in the mullite content of either the kaolin-talc or the kaolin-talc-spinel bodies. The content for both bodies was in the region of 15 ± 5 percent at all times and temperatures.

6. Below 1350°C cordierite formed more rapidly in the kaolin-talc-spinel and kaolin-talc bodies than in the spinel-silica, spinel-silica-excess spinel, and alumina-silica-magnesia bodies. However, due to liquid formation in kaolin-talc bodies at 1350°C and above cordierite formed more rapidly in the spinel-silica, spinel-silica-excess spinel, and alumina-silica-magnesia bodies.

7. The formation of cordierite from silica-spinel and spinel-silica-magnesia apparently involved solid state reaction alone.

8. No significant difference was observed in the cordierite contents or kinetics of the spinel-silica, the spinel-silica-excess spinel, and the alumina-silica-magnesia bodies at any temperature.

Recommendations

Studies should be made of the reaction taking place during the first hour because of the large amounts of cordierite found to form during this time. The effects of different particle sizes on the initial reaction rates should be studied to determine the part played by surface area during the first few minutes of the reaction.

Determining the effects of additions on the rate of formation of cordierite and the firing range in which cordierite forms would be beneficial, particularly in the kaolin-talc bodies since these are the ones used most in industry. Studies should be directed toward the reaction

between kaolin and talc to determine the role of liquid formation in the development of cordierite.

APPENDIX A

RAW MATERIALS

Table 13. Raw Materials Source

Raw Material	Source
Alumina (W. R. Grace & Company
Spinel	W. R. Grace & Company
Magnesia (Reagent Grade)	Fisher Scientific
Silica (Cab-O-Sil)	Cabot Corporation
Kaolin (EPK)	Edgar Plastic Kaolin Div. N. L. Industries
Talc (French)	Talcs de Luzenac

Table 14. Raw Material Particle Size

Raw Material	Particle Size (microns)
Spinel	0.1 - 0.2 ^a
Alumina	0.1 - 0.2 ^a
Magnesia	< 0.5 ^b
Silica	0.007 - 0.014 ^a
Kaolin	3 ^c
Talc	7 ^b

^aParticle size supplied by manufacturer.

^bParticle size taken from SEM photographs; talc appeared to be in platelet form, one micron thick.

^cParticle size supplied by Edgar Plastic Kaolin Div.

Size (microns)	% Less Than
40	100
10	79
5	63
3	51
1	30
0.5	18

Table 15. Chemical Analysis of Edgar Plastic Kaolin

Al_2O_3	38.26
SiO_2	45.58
Fe_2O_3	.70
TiO_2	.42
Li_2O	.15
Na_2O	.11
CaO	.18
K_2O	.33
BaO	.01
ZrO_2	.10
PbO	.02
Cr_2O_3	.01
U_2O_5	.05

APPENDIX B

Table 16. Experimental X-Ray Diffraction Settings

Factor	Setting
Radiation	CuK α
Filter	Nickel
Milliamps	15
Kilovolts	35
Scan Rate	1/4° 2 θ /minute
Scale Factor	1 x 10 ³
Time Constant	4
Chart Speed	1/2 inch/minute

BIBLIOGRAPHY

1. Singer, F. and Cohn, W., "New Stoneware Bodies," Ceramic Abstracts, 8 (11), 824 (1929).
2. Gossner, B. and Mussgnug, F., "Comparative X-Ray Examination of Magnesium Silicates," Ceram. Abstr., 9, 307 (1930).
3. Bragg, W. L., "The Structure of Beryl, $\text{Be}_3\text{Al}_2\text{Si}_6\text{O}_{18}$," Roy. Soc. of London Proc., 111, 691-714 (1926).
4. Byström, A., "The Crystal Structure of Cordierite," Mineralogi och Geologi, 15, 12 (1942).
5. Gibbs, G. V., "The Polymorphism of Cordierite," Am. Mineralogist, 51, 1068-87 (1966).
6. Karkhanavala, M. D. and Hummel, F. A., "The Polymorphism of Cordierite," J. Am. Ceram. Soc., 36, 389-92 (1953).
7. Schreyer, W. and Schairer, J. F., "Composition and Structural States of Anhydrous Mg-Cordierites," J. Petrography, 2, 324-406 (1961).
8. Miyashiro, A., "Cordierite-Indialite Relations," Am. J. Sci., 255, 43-62 (1957).
9. Beals, R. J. and Cook, R. L., "Low Expansion Cordierite Porcelains," J. Am. Ceram. Soc., 35, 53-58 (1952).
10. Lamar, R. S. and Warner, M. J., "Reactions and Fired Property Studies of Cordierite Compositions," J. Am. Ceram. Soc., 37, 602-10 (1954).
11. Jander, W., "Reactions in Solid State at High Temperatures, I.," Z. Anorg. Allgem. Chem., 163, 1-30 (1927).
12. Carter, R. E., "Kinetic Model for Solid-State Reactions," J. Chemical Physics, 34, 2010-15 (1961).
13. Blum, S. L. and Li, P. C., "Kinetics for Nickel Ferrite Formation," J. Am. Ceram. Soc., 44, 611-17 (1961).
14. Bailey, J. T. and Russel, R., "Sintered Spinel Ceramics," B. Am. Ceram. Soc., 47, 1025-29 (1968).

BIBLIOGRAPHY (Concluded)

15. Zirczy, N., "Kinetics of Cordierite Formation," Master's Thesis, School of Ceramic Engineering, Georgia Institute of Technology, August 1972.
16. Aza, S. and Espinosa, J., "Mechanism of Cordierite Formation in Ceramic Bodies," Bol. Soc. Espan. Ceram. II (5), 315-321 (1972).
17. Klug, H. and Alexander, L., X-Ray Diffraction Procedure, John Wiley and Sons, Inc., New York, 1954, pp. 415-428.
18. Bronson, D., "Kinetics and Mechanism of the Reaction Between Zinc Oxide and Aluminum Oxide," J. Am. Ceram. Soc., 48, 591-595 (1965).